Non-diffusive relaxation of a transient thermal grating analyzed with the Boltzmann transport equation

Citation: Collins, Kimberlee C. et al. "Non-Diffusive Relaxation of a Transient Thermal Grating Analyzed with the Boltzmann Transport Equation." Journal of Applied Physics 114, 10 (September 2013): 104302 © 2013 AIP Publishing LLC

As Published: http://dx.doi.org/10.1063/1.4820572

Publisher: American Institute of Physics (AIP)

Persistent URL: http://hdl.handle.net/1721.1/118931

Version: Final published version: final published article, as it appeared in a journal, conference proceedings, or other formally published context

Non-diffusive relaxation of a transient thermal grating analyzed with the Boltzmann transport equation

Kimberlee C. Collins,[1] Alexei A. Maznev,[2] Zhiting Tian,[1] Keivan Esfarjani,[3] Keith A. Nelson,[2] and Gang Chen[1,a)]

[1]*Department of Mechanical Engineering, Massachusetts Institute of Technology, Cambridge, Massachusetts 02139, USA*
[2]*Department of Chemistry, Massachusetts Institute of Technology, Cambridge, Massachusetts 02139, USA*
[3]*Department of Mechanical and Aerospace Engineering, Rutgers University, Piscataway, New Jersy 08854, USA*

(Received 5 June 2013; accepted 22 August 2013; published online 10 September 2013)

The relaxation of an one-dimensional transient thermal grating (TTG) in a medium with phonon-mediated thermal transport is analyzed within the framework of the Boltzmann transport equation (BTE), with the goal of extracting phonon mean free path (MFP) information from TTG measurements of non-diffusive phonon transport. Both gray-medium (constant MFP) and spectrally dependent MFP models are considered. In the gray-medium approximation, an analytical solution is derived. For large TTG periods compared to the MFP, the model yields an exponential decay of grating amplitude with time in agreement with Fourier's heat diffusion equation, and at shorter periods, phonon transport transitions to the ballistic regime, with the decay becoming strongly non-exponential. Spectral solutions are obtained for Si and PbSe at 300 K using phonon dispersion and lifetime data from density functional theory calculations. The spectral decay behaviors are compared to several approximate models: a single MFP solution, a frequency-integrated gray-medium model, and a "two-fluid" BTE solution. We investigate the utility of using the approximate models for the reconstruction of phonon MFP distributions from non-diffusive TTG measurements. © *2013 AIP Publishing LLC*.
[http://dx.doi.org/10.1063/1.4820572]

I. INTRODUCTION

Lattice thermal conductivity exhibits non-diffusive characteristics over length scales comparable to phonon mean free paths (MFPs). Information on phonon MFP distributions within materials is important for understanding and engineering heat transport, which has prompted recent experiments[1–7] to investigate phonon-mediated thermal transport at small length scales. Experiments and theory have shown that in materials such as Si, the Fourier law breaks down at much longer distances than previously thought, on the order of microns at room temperature.[6–10] When temperature gradients occur at length scales comparable to the MFP of heat carrying phonons, the diffusion model of thermal conductivity becomes inadequate, even in the absence of physical boundaries.[11,12] In the non-diffusive regime, phonon transport can be described by the Boltzmann transport equation (BTE), which is difficult to solve. In the past, theoreticians have resorted to the gray-medium (constant MFP) approximation and to idealized geometries that do not match experimental conditions, such as one-dimensional transport across a slab bounded by blackbody walls.[13–16]

One notable experimental method for measuring thermal conductivity is the transient thermal grating (TTG) technique.[17–19] The TTG technique uses crossed laser beam interference to produce a spatially sinusoidal temperature profile in a sample, as illustrated in Fig. 1, which gives rise to a spatially modulated refractive index. The subsequent decay of the temperature profile is measured using a diffracted probe beam. The heat transfer distance in a TTG experiment is controlled by the grating period, L, which can be easily varied over a wide range. Non-diffusive phonon transport has been observed when L is within the range of MFPs of the heat carrying phonons in a material.[6] The simple geometry, the absence of material interfaces, and the sinusoidal temperature profile make the TTG arrangement attractive for theoretical analysis. Maznev *et al.*[20] obtained an analytical solution for the one-dimensional TTG relaxation using a "two-fluid" approximation that combined the diffusion model for the high frequency part of the phonon spectrum and the BTE for low frequency phonons. Minnich[21] used the result of Ref. 20, along with a solution to the BTE obtained with a deviational Monte Carlo method,[22] to propose a procedure for reconstructing phonon MFP distributions from TTG data.

In this article, we present a systematic study of BTE solutions to the one-dimensional TTG problem. We start by analyzing the gray-medium model, assuming a constant phonon MFP, for which we obtain an analytical solution. We proceed with numerical solutions to the spectral phonon BTE for Si and PbSe at 300 K, including all six phonon branches, using phonon dispersions and relaxation times obtained from density functional theory (DFT) calculations.[9,23] We then compare the exact spectral BTE solutions with approximate solutions, including the gray-medium model and the two-fluid model from Ref. 20, and consider

a)gchen2@mit.edu

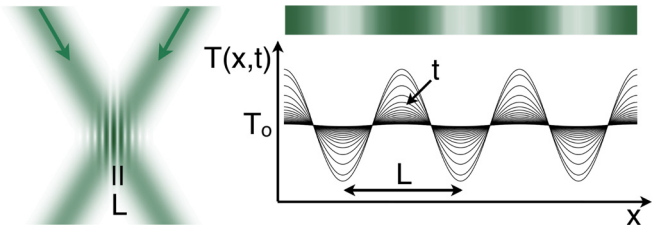

FIG. 1. Illustration of a TTG experiment, in which crossed pump lasers produce a sinusoidal interference pattern on the surface of a sample with period L. The interference pattern results in a spatially sinusoidal temperature profile that decays in time.

the utility of those approximate models for reconstructing phonon MFP distributions from TTG measurements of non-diffusive thermal transport.

II. GRAY-MEDIUM MODEL

We consider the thermal relaxation of a one-dimensional, spatially sinusoidal temperature profile, as illustrated in Fig. 1. Our formulation differs from the experimental geometry of Ref. 6, where heat transport was influenced by the boundary scattering in a thin membrane. Rather, our approach is appropriate for TTG measurements in bulk materials, where the depth of the thermal grating is much greater than the grating period.[17] In order to extend this approach to thin membranes or strongly absorbing materials in which heat is dissipated into the depth of a sample, a multidimensional BTE would need to be considered. Initially, the temperature profile is given by

$$T(x,t=0) = T_{max}\cos(qx), \tag{1}$$

where T is the temperature deviation from T_o, the average background temperature, T_{max} is the peak temperature deviation, t is time, x is the spatial variable, and q is the spatial wave vector, which relates to the grating period through $q = 2\pi/L$. The heat diffusion equation yields an exponential thermal decay of the form

$$T(x,t) = T_{max}\cos(qx)e^{-\alpha q^2 t}, \tag{2}$$

where α is the thermal diffusivity of the material. At sufficiently small grating periods, the thermal transport will be non-diffusive and needs to be described instead by the phonon BTE. In the relaxation time approximation, the phonon BTE takes the form[13,24]

$$\frac{\partial g}{\partial t} + \mu v\frac{\partial g}{\partial x} = \frac{g_o - g}{\tau}, \tag{3}$$

$$g_o = \frac{1}{4\pi}\hbar\omega D(\omega) f_{BE}(T) \approx \frac{1}{4\pi}C_\omega T, \tag{4}$$

where our distribution function, $g = g(x,t,\mu)$, is phonon energy density per unit frequency interval per unit solid angle, equal to the occupation function, f, multiplied by $\hbar\omega D(\omega)/4\pi$, $g_o = g_o(x,t)$ is the distribution when f is the equilibrium occupation function determined by the Bose-Einstein distribution, $f_{BE}(T)$, $\mu = \cos(\theta)$ is the directional cosine, v is phonon group velocity, τ is phonon relaxation time, $\hbar$ is the reduced Planck constant, ω is phonon frequency, $D(\omega)$ is phonon density of states, and C_ω is the differential, frequency-dependent specific heat. Again, both g and f are defined as deviations from the average background values corresponding to thermal equilibrium at the background temperature, T_o. In the small perturbation limit, the equilibrium distribution function, g_o, is proportional to the temperature change, as shown in Eq. (4).[10] In the gray-medium model, v and τ are assumed to be constant, in which case the BTE does not depend on phonon frequency, and the frequency dependence of g can be ignored.

We seek a spatially periodic solution for g by assuming that g and T are of the form $\tilde{g}(t,\mu)\exp(iqx)$ and $\tilde{T}(t)\exp(iqx)$. Now Eq. (3) takes the form of a first-order ordinary differential equation for $\tilde{g}$,

$$\frac{\partial\tilde{g}}{\partial t} + \gamma\tilde{g} = \frac{\tilde{g}_o}{\tau}, \tag{5}$$

with the solution

$$\tilde{g}(t,\mu) = \frac{1}{\tau}\int_0^t e^{\gamma(t'-t)}\tilde{g}_o(t')dt' + Ae^{-\gamma t}, \tag{6}$$

where $\gamma = (1 + iq\mu v\tau)/\tau$ and $A = \tilde{g}(t=0,\mu) = \tilde{g}_o(0)$. We obtain a second relation between $\tilde{g}$ and $\tilde{g}_o$ using energy conservation, assuming a gray medium,[13]

$$g_o(x,t) = \frac{1}{2}\int_{-1}^{1} g(x,t,\mu)d\mu, \tag{7}$$

which leads to

$$\tilde{g}_o(t) = \tilde{g}_o(0)\,\mathrm{sinc}(qvt)e^{-t/\tau} + \frac{1}{\tau}\int_0^t \tilde{g}_o(t')e^{(t'-t)/\tau}\,\mathrm{sinc}(qv(t'-t))dt'. \tag{8}$$

We can further generalize Eq. (8) by substituting nondimensional variables,

$$\zeta = \frac{t}{\tau}, \quad \eta = qv\tau = \frac{2\pi\Lambda}{L}, \quad \Upsilon = \frac{\tilde{g}_o(t)}{\tilde{g}_o(0)} = \frac{\tilde{T}(t)}{\tilde{T}(0)}, \tag{9}$$

producing

$$\Upsilon(\zeta) = \mathrm{sinc}(\eta\zeta)e^{-\zeta} + \int_0^\zeta \Upsilon(\zeta')\mathrm{sinc}(\eta(\zeta'-\zeta))e^{(\zeta'-\zeta)}d\zeta', \tag{10}$$

which is a nondimensional solution of the gray-medium, one-dimensional phonon BTE for a sinusoidal temperature profile. Here, Λ is the phonon MFP, which relates to relaxation time and group velocity through $\Lambda = v\tau$. Equation (10) is a Volterra integral equation of the second kind, which can be solved using standard numerical techniques.[25]

The solution of the diffusion equation, given by Eq. (2), can be represented in a similar nondimensional form

$$\Upsilon(\zeta) = e^{-\beta\zeta}, \tag{11}$$

where $\beta = \alpha q^2\tau$.

An alternate approach for deriving an analytical solution to the one-dimensional, gray-medium phonon BTE for a sinusoidal temperature profile assumes a spatially periodic solution for g and utilizes a Fourier transform in time. Starting with the gray-medium phonon BTE with a spatially periodic instantaneous source,

$$\frac{\partial g}{\partial t} + \mu v \frac{\partial g}{\partial x} = \frac{g_o - g}{\tau} + A\delta(t)e^{iqx}, \tag{12}$$

assuming a periodic spatial solution of the form, $\exp(iqx)$, and taking a Fourier transform in time leads to

$$-i\nu\tilde{\tilde{g}} + iqv\mu\tilde{\tilde{g}} = \frac{\tilde{\tilde{g}}_o - \tilde{\tilde{g}}}{\tau} + A, \tag{13}$$

where $\tilde{\tilde{g}} = \tilde{\tilde{g}}(\mu) = \int \tilde{g}(t,\mu)e^{i\nu t}dt$. Integrating over μ to satisfy energy conservation, as shown in Eq. (7), gives

$$\tilde{\tilde{g}}_o = \frac{A\tau}{q\Lambda\left(\tan^{-1}\left(\frac{q\Lambda}{1-i\nu\tau}\right)\right)^{-1} - 1}, \tag{14}$$

which is an analytical solution for the equilibrium distribution function in the frequency domain. To obtain a time domain solution, an inverse Fourier transform can be performed numerically,

$$\tilde{g}_o = \frac{A\tau}{2\pi}\int_{-\infty}^{\infty} \frac{\exp(-i\nu t)}{q\Lambda\left(\tan^{-1}\left(\frac{q\Lambda}{1-i\nu\tau}\right)\right)^{-1} - 1} d\nu. \tag{15}$$

Writing Eq. (15) in the nondimensional variables of Eq. (9) leads to

$$\Upsilon(\zeta) = \frac{1}{2\pi}\int_{-\infty}^{\infty} \frac{\exp(-i\psi\zeta)}{\eta\left(\tan^{-1}\left(\frac{\eta}{1-i\psi}\right)\right)^{-1} - 1} d\psi, \tag{16}$$

where $\psi = \nu\tau$.

Equations (10) and (16) produce identical decay curves. A few numerically computed solutions of $\Upsilon(\zeta)$ for different values of η are shown in Fig. 2(a). The decay curves shown correspond to the difference between the peak and null temperatures in the sinusoidal temperature profile as a function of time. These are compared to corresponding diffusion model solutions from Eq. (11). In the diffusive limit, $\alpha_{bulk} = v\Lambda/3$ and $\beta_{bulk} = \eta^2/3$. The diffusive limit curves yield faster decays than the corresponding BTE curves, indicating that the thermal transport at small length scales slows down compared to Fourier law predictions.[10,12,13,20,24]

At large η values, the decay becomes strongly non-exponential and acquires an oscillatory character. The thermal decay for very large η values approaches the ballistic limit, as shown in Fig. 2(b). In the ballistic limit, $\tau \to \infty$, and Eq. (8) reduces to $\Upsilon = \mathrm{sinc}(\eta\zeta)$. We can understand this oscillatory behavior by considering the case of purely ballistic transport, which would be equivalent to having non-interacting particles moving with a constant velocity, v, and having an initial density distribution, $\cos(qx)$. For a subset of particles whose velocity makes an angle θ with the x direction, the particle density will oscillate as $\cos(qx - qv\mu t)$. Integrating over all angles yields a sinc function in time, identical to the ballistic limit derived from the BTE.

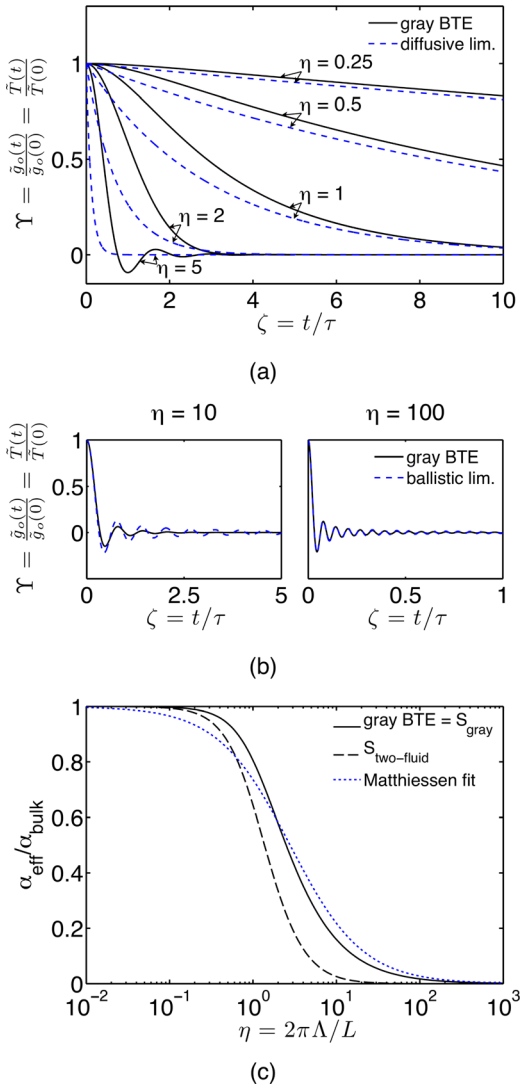

FIG. 2. (a) Gray-medium, nondimensional BTE thermal decay curves, $\Upsilon(\zeta = t/\tau) = \tilde{g}_o(t)/\tilde{g}_o(0) = \tilde{T}(t)/\tilde{T}(0)$, for different nondimensional length scales, $\eta = 2\pi\Lambda/L$, compared to corresponding diffusive Fourier decay curves and best fit Fourier decay curves. (b) BTE decay curves for large η values compared to the ballistic limit. (c) Normalized gray-medium effective thermal diffusivity for a range of η (solid line). The suppression function from Ref. 20 is shown for comparison (dashed line). A fit by Matthiessen's rule given by Eq. (18), where $L_{eff} = L/2.254$, is shown (dotted line).

It is instructive to find the dependence of the "effective" thermal diffusivity on the TTG period by fitting the BTE curves using diffusion model solutions, as is frequently done in the analysis of experimental data.[5,6] The Fourier curves in Fig. 2(a) are fit to the BTE curves by varying β, and example fitted curves are shown. This produces a set of effective values of β, which are normalized and plotted in Fig. 2(c). In the limit of small η, which corresponds to large grating periods, transport is in the diffusive regime, with $\beta_{eff}/\beta_{bulk} = 3\beta_{eff}/\eta^2 = \alpha_{eff}/\alpha_{bulk} = 1$, and Fourier fits are good. At progressively larger values of η, the transport transitions to the ballistic regime, with BTE curves displaying highly

non-exponential behavior which cannot be captured by the fitted Fourier curves, and the effective diffusivity approaches zero. We would like to stress that this result does not mean that ballistic phonons do not carry heat; they simply transfer much less heat than diffusion theory predicts.

The effective thermal diffusivity falls off by a factor of two at $\Lambda = L/2.513$, which is close to the TTG peak-to-null distance, $L/2$. One may want to attempt to use Matthiessen's rule by analogy with other size-effects,[24] even though in our case there is no scattering process associated with the length scale L. If one follows a Matthiessen's rule approach, where L_{eff} is the effective length scale in the problem,

$$\frac{1}{\Lambda_{eff}} = \frac{1}{\Lambda_{bulk}} + \frac{1}{L_{eff}}, \tag{17}$$

and rearranging gives

$$\frac{\Lambda_{eff}}{\Lambda_{bulk}} = \left(1 + \frac{\Lambda_{bulk}}{L_{eff}}\right)^{-1}, \tag{18}$$

which can be fit to the gray BTE curve in Fig. 2(c) to find Leff. The best fit curve is plotted in Fig. 2(c), and suggests an effective length scale of $L_{eff} = L/2.254$, which is again close to L/2. However, Eq. (18) yields a poor fit to the BTE result and, moreover, lacks a sound physical meaning, because the thermal grating does not physically reduce the phonon MFP.

III. SPECTRAL MODEL

Heat carrying phonons in real materials have a wide range of MFPs,[6–10] rendering the gray-medium model inadequate. In the spectral model, phonon group velocity, v, and relaxation time, τ, in Eq. (3) become frequency-dependent, and hence, g should now be treated as a function of four variables, $g = g(x, t, \mu, \omega)$. Our model includes phonon dispersions and lifetimes for all six phonon branches as a function of frequency, obtained through DFT calculations for Si and PbSe at 300 K.[9,23] Si and PbSe are interesting case materials to consider due to their different thermal conductivity accumulation functions. Si has a thermal conductivity accumulation function spanning a wide range of MFPs, from 10 nm to 10 μm,[9] while PbSe has a much more narrow distribution.[23] We used Brillouin-zone-averaged properties, thus assuming an isotropic medium. We verified that our averaging produced literature values for the thermal conductivities and the volumetric specific heats of Si and PbSe at 300 K.

As in the gray-medium case, we assume a spatial dependence of the phonon distribution and temperature of the form $\exp(iqx)$, producing

$$\frac{\partial \tilde{g}}{\partial t} + iq\mu v\tilde{g} = \frac{\tilde{g}_o - \tilde{g}}{\tau}, \tag{19}$$

$$\tilde{g}_o(\tilde{T}) \approx \frac{1}{4\pi} C_\omega \tilde{T}, \tag{20}$$

where the temperature variation is given by[10]

$$\tilde{T} = \frac{2\pi}{\int_0^{\omega_m} \frac{C_\omega}{\tau} d\omega} \int_0^{\omega_m} \int_{-1}^{1} \frac{\tilde{g}}{\tau} d\mu d\omega. \tag{21}$$

Our numerical solution of Eqs. (19)–(21) uses an explicit finite difference scheme. The granularity used for the variables in the finite difference solution included at least 32 bins for μ and 100 bins for ω, with $dt \leq 2$ ps. Convergence was verified by systematically increasing granularity. We further verified our spectral BTE code by inputting gray-medium parameters and achieving identical results to the gray-medium model discussed previously.

Calculated thermal decay curves for a range of grating periods in Si are shown in Fig. 3(a), and compared to diffusive Fourier heat equation solutions. The BTE curves decay slower than the Fourier curves, indicating that thermal transport deviates from the diffusive regime, even for grating periods as large as $L = 20\,\mu$m. The Fourier curves are fit to the BTE curves by varying α, producing a set of effective values of α as a function of L, which are normalized and plotted as closed symbols in Fig. 3(b) for Si and Fig. 3(c) for PbSe.

Now that we have computed a spectral BTE solution, we can compare it to approximate models. We start with the most crude approach: assuming a single MFP. Normally, MFP estimates are obtained from the experimental values of thermal diffusivity using the expression, $\alpha_{bulk} = v\Lambda/3$, given by the gray-medium BTE, and assuming the Debye model in which v is the branch-average acoustic velocity.[24] This approach yields MFP values of ~40 nm for Si[8,24] and ~2 nm for PbSe,[23,26] but these produce effective diffusivity curves shifted towards much lower grating periods than our spectral BTE calculations. It has been suggested that the gray-medium BTE can be made to work better for Si by using a larger MFP value.[7,8,27] We find that the best fit to the spectral BTE results for Si is achieved with a MFP as large as 1 μm, and even then the fit is quite poor, as can be seen from the dotted line in Fig. 3(b). For PbSe, a MFP of 6.5 μm yields a somewhat better fit to the spectral BTE results, as shown in Fig. 3(c).

We can improve on the single-MFP model by assuming that phonons of frequency ω, for a given phonon branch, contribute to the thermal conductivity according to the gray-medium model with MFP $\Lambda(\omega)$. The effective thermal conductivity, k_{eff}, is found by summing over the phonon spectrum as follows:

$$\kappa = \frac{k_{eff}}{k_{bulk}} = \frac{1}{3k_{bulk}} \int_0^{\omega_{max}} S_{gray} C_\omega v \Lambda d\omega, \tag{22}$$

where the suppression function, $S_{gray} = \alpha_{eff}/\alpha_{bulk}$, is given by the solid curve in Fig. 2(c). This approach might be reasonable if phonons of different frequencies did not interact such that phonons at each frequency, for a given phonon branch, obeyed the gray-medium BTE. At room temperature, phonon scattering is dominated by phonon-phonon interactions, in which case Eq. (22) lacks a solid foundation. Nevertheless, one can hope that it will yield an improvement over the single-MFP gray-medium model, and indeed we

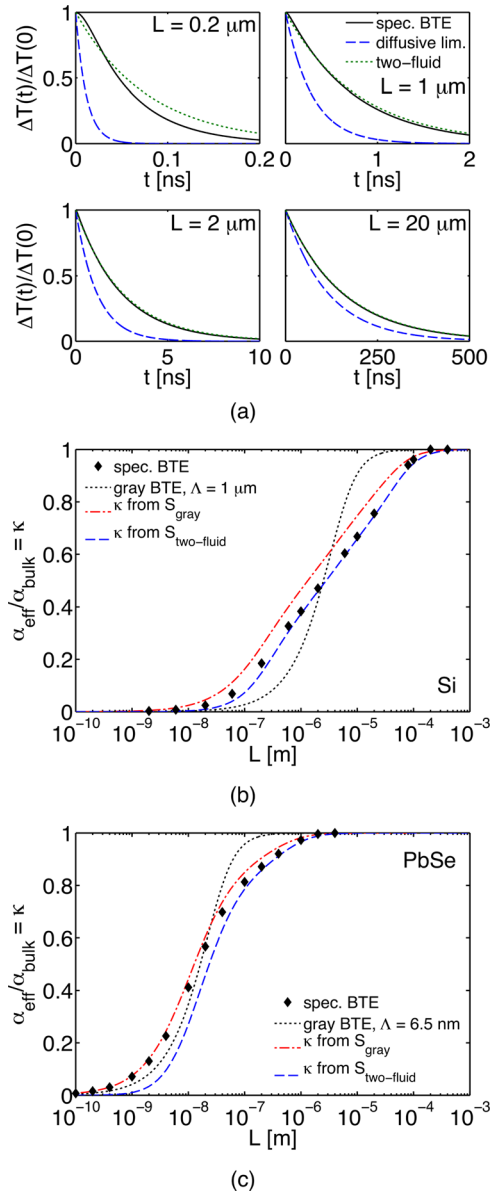

FIG. 3. Spectral BTE solutions showing (a) normalized BTE temperature decay curves (solid lines) for Si for different grating periods, L, compared to corresponding diffusive Fourier decays (dashed lines) and exponential TTG decays based on the model in Ref. 20 (dotted lines). ΔT is the difference in the peak and null of the TTG temperature profile. Normalized effective thermal conductivities (closed symbols), κ, are shown for a range of L, for (b) Si and (c) PbSe. Suppression functions based on our frequency-integrated gray-medium BTE approach (dash-dotted lines) and from Ref. 20 (dashed lines) are used to predict κ for comparison, and single-MFP model fits (dotted lines) are also shown.

observe that this "frequency-integrated gray-medium" approach does yield better results, as shown by the dash-dotted lines in Figs. 3(b) and 3(c). In fact, for PbSe, the dependence of the effective diffusivity on grating period is reasonably reproduced over a wide range of grating periods.

Now let us consider the approximate solution to the spectral BTE derived in Ref. 20. The model[20] analyzes the onset of non-diffusive transport when the TTG period is much larger than the MFPs of high-frequency phonons responsible for most of the specific heat. Accordingly, those high-frequency phonons are assumed to obey the diffusion model, whereas the low-frequency phonons are analyzed with the BTE. Within this two-fluid approach, it was found that the TTG decay remains exponential, as in Eq. (2), with the thermal conductivity modified by a suppression function as follows:

$$\kappa = \frac{k_{eff}}{k_{bulk}} = \frac{1}{3k_{bulk}} \int_0^{\omega_{max}} S_{two-fluid} C_\omega v \Lambda d\omega, \tag{23}$$

$$S_{two-fluid} = \frac{3}{\eta^2}\left(1 - \frac{\tan^{-1}\eta}{\eta}\right). \tag{24}$$

In Fig. 3(a), the exponential TTG decay curves according to Ref. 20 for Si are compared to the spectral BTE solutions. The agreement is quite good down to $L = 1\ \mu$m, where the spectral BTE yields a nearly exponential decay, and remains reasonable even at $L = 0.2\ \mu$m. The dashed line in Fig. 3(b) shows that for Si at 300 K, the dependence of the effective diffusivity on TTG period according to Ref. 20 closely matches the spectral BTE results. In Ref. 20, it was suggested that for Si at 300 K, the approximate solution would be expected to work for $L > 1\ \mu$m. We see that in fact it works quite well for a much wider range of TTG periods.

IV. CONSIDERATIONS FOR MFP SPECTROSCOPY

Solutions to the phonon BTE can be used to extract phonon MFP information from measurements of non-diffusive phonon transport. The MFP distribution of heat-carrying phonons can be characterized by the thermal conductivity accumulation function versus MFP, which has been shown to be instrumental for analyzing thermal transport in bulk materials and nanostructures.[28,29] Minnich[21] recently suggested a way to reconstruct the thermal conductivity accumulation function, $\Phi(\Lambda)$, as a function of phonon MFP, Λ, using non-diffusive measurements of normalized effective thermal conductivity, κ, and an appropriate suppression function, S, as follows:

$$\kappa = \int_0^\infty S(\eta)\phi(\Lambda)d\Lambda = \int_0^\infty -\frac{dS}{d\eta}\frac{d\eta}{d\Lambda}\Phi(\Lambda)d\Lambda. \tag{25}$$

Here the thermal conductivity accumulation function, $\Phi(\Lambda)$, is related to the thermal conductivity per MFP, $\phi(\Lambda)$, through $\Phi(\Lambda) = \int_0^\Lambda \phi(\Lambda')d\Lambda'$. A similar equation appears in the analysis of thermal conductivity size effects in nanostructures, with the nanostructure dimension taking the place of the thermal grating period, L.[29] The extraction of $\Phi(\Lambda)$ from the measured dependence of κ on L is essentially the inverse of the methods discussed above for predicting effective thermal conductivity using a suppression function and a known MFP distribution. Even though such a reconstruction is an ill-posed problem, given the limited number of κ measurements, progress can be made if certain constraints are imposed on $\Phi(\Lambda)$. Minnich[21] showed that if $\Phi(\Lambda)$ is a smooth function that monotonically increases from 0 to 1, convex optimization[30,31] can be used to reasonably estimate $\Phi(\Lambda)$.

Following Minnich's approach, we reconstruct the thermal conductivity accumulation functions for Si and PbSe at

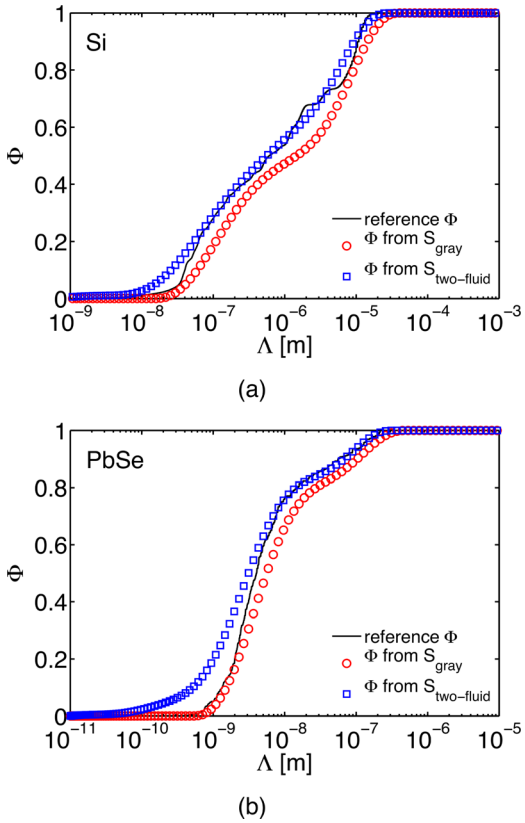

FIG. 4. Reconstructed thermal conductivity accumulation functions (open symbols) as a function of phonon MFP for (a) Si and (b) PbSe at 300 K. Solid curves were calculated based on Refs. 9 and 23. Spectral BTE normalized effective thermal conductivity, κ, values were used as inputs for the reconstructions, along with suppression functions from Ref. 20 (open squares) and from our frequency-integrated gray-medium approach (open circles).

300 K. The resulting reconstructions are shown in Figs. 4(a) and 4(b). We use the effective κ values obtained with the spectral BTE as the "measurement" inputs for Eq. (25). We compare reconstructions achieved using the suppression function from Ref. 20 and the suppression function from our frequency-integrated gray-medium approach, to reference $\Phi(\Lambda)$ distributions calculated from the same DFT dispersion and relaxation time data[9,23] which we used for our spectral BTE calculations. As expected from the results of the forward method plotted in Figs. 3(b) and 3(c), using $S_{two-fluid}$ produces a better MFP distribution reconstruction for Si and using S_{gray} produces a reasonable reconstruction for PbSe. The approximations in the two-fluid approach of Ref. 20 lead to a more accurate result for low-frequency, long MFP phonons, and indeed, we observe that the two-fluid model well reproduces the long MFP thermal conductivity accumulation function for both Si and PbSe. Our frequency-integrated gray-medium approach is more appropriate for materials that approximate gray-mediums with step-like thermal conductivity accumulation functions, and hence, works better for PbSe than for Si.

V. SUMMARY

We have presented gray-medium and spectral solutions to the one-dimensional phonon BTE corresponding to the spatially sinusoidal temperature profile in a TTG experiment. Our gray-medium analysis yielded an analytical solution which approached the diffusive limit for grating periods that were large compared to the gray-medium phonon MFP, and approached the ballistic limit for small grating periods. Spectral BTE solutions were found for Si and PbSe at 300 K using phonon dispersions and lifetimes for all six phonon branches from DFT calculations. We compared the spectral BTE decays to several approximate models: a single-MFP BTE solution, a frequency-integrated gray-medium BTE model, and a two-fluid model from Ref. 20 that combines the BTE with the diffusion equation. We found that the spectral BTE results for Si were well reproduced by the two-fluid model from Ref. 20, and that PbSe was reasonably modeled using our proposed frequency-integrated gray-medium BTE approach. We also considered the inverse problem of reconstructing thermal conductivity accumulation functions from measured effective thermal conductivities and modeled suppression functions. While the suppression function from Ref. 20 produced better results for Si, the suppression function from our frequency-integrated gray-medium BTE approach produced reasonable results, and, in fact, worked better for PbSe. We anticipate that the latter approach, applied to different experimental geometries, may offer reasonable estimations for modeling non-diffusive thermal transport, and extracting phonon spectral information from experimental measurements.

ACKNOWLEDGMENTS

The authors gratefully acknowledge helpful discussions with Professor Austin Minnich. We are also grateful to Dr. Jivtesh Garg for his help with averaging DFT values for Si. This work is primarily supported by the "Solid State Solar-Thermal Energy Conversion Center (S^3TEC)," an Energy Frontier Research Center funded by the U.S. Department of Energy, Office of Science, Office of Basic Energy Sciences, under Award No. DE-SC0001299/DE-FG02-09ER46577 (TTG and MFP spectroscopy), and by MIT-KFUMP Clean Water and Clean Energy Center (on BTE solution).

[1]P. G. Sverdrup, S. Sinha, M. Asheghi, S. Uma, and K. E. Goodson, Appl. Phys. Lett. **78**, 3331 (2001).
[2]Y. K. Koh and D. G. Cahill, Phys. Rev. B **76**, 075207 (2007).
[3]M. E. Siemens, Q. Li, R. Yang, K. A. Nelson, E. H. Anderson, M. M. Murnane, and H. C. Kapteyn, Nature Mater. **9**, 26 (2010).
[4]A. J. Minnich, J. A. Johnson, A. J. Schmidt, K. Esfarjani, M. S. Dresselhaus, K. A. Nelson, and G. Chen, Phys. Rev. Lett. **107**, 095901 (2011).
[5]J. A. Johnson, A. A. Maznev, M. T. Bulsara, E. A. Fitzgerald, T. C. Harman, S. Calawa, C. J. Vineis, G. Turner, and K. A. Nelson, J. Appl. Phys. **111**, 023503 (2012).
[6]J. A. Johnson, A. A. Maznev, J. Cuffe, J. K. Eliason, A. J. Minnich, T. Kehoe, C. M. S. Torres, G. Chen, and K. A. Nelson, Phys. Rev. Lett. **110**, 025901 (2013).
[7]K. T. Regner, D. P. Sellan, Z. Su, C. H. Amon, A. J. H. McGaughey, and J. A. Malen, Nat. Commun. **4**, 1640 (2013).
[8]A. S. Henry and G. Chen, J. Comput. Theor. Nanosci. **5**, 141 (2008).
[9]K. Esfarjani, G. Chen, and H. T. Stokes, Phys. Rev. B **84**, 085204 (2011).
[10]A. J. Minnich, G. Chen, S. Mansoor, and B. S. Yilbas, Phys. Rev. B **84**, 235207 (2011).
[11]C. L. Tien and G. Chen, J. Heat Transfer **116**, 799 (1994).
[12]G. Chen, J. Heat Transfer **118**, 539 (1996).

[13]A. Majumdar, J. Heat Transfer **115**, 7 (1993).
[14]S. V. J. Narumanchi, J. Y. Murthy, and C. H. Amon, J. Heat Transfer **126**, 946 (2004).
[15]A. Mittal and S. Mazumder, J. Heat Transfer **132**, 052402 (2010).
[16]D. P. Sellan, J. E. Turney, A. J. H. McGaughey, and C. H. Amon, J. Appl. Phys. **108**, 113524 (2010).
[17]H. J. Eichler, P. Günter, and D. W. Pohl, *Laser-Induced Dynamic Gratings* (Springer-Verlag, Berlin, 1986), Vol. 50.
[18]J. A. Rogers, Y. Yang, and K. A. Nelson, Appl. Phys. A **58**, 523 (1994).
[19]J. A. Rogers, A. A. Maznev, M. J. Banet, and K. A. Nelson, Annu. Rev. Mater. Sci. **30**, 117 (2000).
[20]A. A. Maznev, J. A. Johnson, and K. A. Nelson, Phys. Rev. B **84**, 195206 (2011).
[21]A. J. Minnich, Phys. Rev. Lett. **109**, 205901 (2012).
[22]J.-P. M. Péraud and N. G. Hadjiconstantinou, Phys. Rev. B **84**, 205331 (2011).
[23]Z. Tian, J. Garg, K. Esfarjani, T. Shiga, J. Shiomi, and G. Chen, Phys. Rev. B **85**, 184303 (2012).
[24]G. Chen, *Nanoscale Energy Transport and Conversion* (Oxford University Press, Inc., 2005).
[25]W. Press, *Numerical Recipes in Fortran 77: The Art of Scientific Computing, Fortran Numerical Recipes* (Cambridge University Press, 1992).
[26]H. Wang, Y. Pei, A. D. LaLonde, and G. J. Snyder, Adv. Mater. **23**, 1366 (2011).
[27]Y. Ju and K. Goodson, Appl. Phys. Lett. **74**, 3005 (1999).
[28]C. Dames and G. Chen, *Thermoelectrics Handbook: Macro to Nano*, edited by D. M. Rowe (Taylor & Francis Group, 2006).
[29]F. Yang and C. Dames, Phys. Rev. B **87**, 035437 (2013).
[30]M. Grant and S. Boyd, CVX: Matlab software for disciplined convex programming, version 2.0 beta, CVX Research, Inc., 2012, see http://cvxr.com/cvx.
[31]M. Grant and S. Boyd, in *Recent Advances in Learning and Control, Lecture Notes in Control and Information Sciences*, edited by V. Blondel, S. Boyd, and H. Kimura (Springer-Verlag Limited, 2008), pp. 95–110.